APPLICATIONS OF PERTURBATION THEORY TO ACOUSTIC LOGGING

by

K. J. Ellefsen and C. H. Cheng

Earth Resources Laboratory
Department of Earth, Atmospheric, and Planetary Sciences
Massachusetts Institute of Technology
Cambridge, MA 02139

ABSTRACT

For guided wave propagation in boreholes, perturbation theory is used to calculate (1) the partial derivative of the wavenumber or frequency with respect to an elastic modulus or density, (2) group velocity, and (3) the effect of a borehole with a slightly irregular cross section upon the phase velocity. The method, which is developed for a fluid-filled, cylindrical borehole through a transversely isotropic formation, relates perturbations in formation properties (i.e., elastic moduli, densities, and interface locations) and wave properties (i.e., wavenumber and frequency) for guided waves with any azimuthal order number. Velocity perturbations, which are calculated for three common cross sections of irregular boreholes, show several general characteristics. The tube and pseudo-Rayleigh waves, which have no azimuthal dependence, completely smooth the effects of the irregularity making the velocity perturbation independent of the wave's orientation. The perturbations for the tube wave are small because it is a Stoneley wave, but those for the pseudo-Rayleigh wave are much larger because the borehole shape affects the multiply-reflected part of this wave. The velocity perturbations for the flexural and screw waves are similar in character to those for the pseudo-Rayleigh wave, but because these waves are directional, they can interact with the irregularity to amplify or diminish the velocity perturbation.

INTRODUCTION

The continental and ocean drilling programs and the oil industry use logging methods to determine the in-situ properties of rocks. When acoustic logging is performed, the guided waves provide information about S-wave velocity, transverse isotropy, fracturing, and permeability. To successfully use these guided waves to evaluate formation properties, a robust method of calculating a Jacobian and a thorough understanding of their behavior in actual boreholes are necessary. As part of this effort, we have applied

perturbation theory to address three different aspects of guided wave propagation.

The first application is calculating partial derivatives which are needed in an inversion for formation properties. Cheng et al. (1982), Stevens and Day (1986), and Burns and Cheng (1987), have used perturbation theory to calculate partial derivatives because numerical derivatives can sometimes be inaccurate. Their results only pertain to derivatives at constant wavenumber for tube and pseudo-Rayleigh waves in isotropic formations. Several new developments in acoustic logging suggest that their work should be developed further: recently published data (see e.g., Thomsen (1986) or Winterstein (1986)) indicate that many sedimentary formations are transversely isotropic, array processing of data obtained by multi-receiver tools yields estimates of the wavenumber and attenuation coefficient at constant frequency, and several new logging tools generate flexural and screw waves. For these reasons, we shall present a method of calculating partial derivatives for all guided waves in transversely isotropic formations at either constant frequency or constant wavenumber.

The second application is calculating group velocity. Because numerical differentiation of the dispersion curves can give poor results, Toksöz et al. (1984) used perturbation theory to calculate the group velocities of tube and pseudo-Rayleigh waves in isotropic formations. Motivated by the same reasons which we previously mentioned, we shall present a method of calculating group velocity for all guided waves in transversely isotropic formations.

The third application is estimating the change in the phase velocity of a guided wave due to a borehole with a slightly irregular cross section. Since all boreholes are slightly irregular, this issue must be addressed before the dispersion curves are used to estimate formation properties. Furthermore, because the long axis of an elliptical borehole can sometimes be correlated with the horizontal components of the stress (Zoback, 1983), an interesting question is whether the guided waves can be used to detect this ellipticity. Willen (1983) used a perturbative method to calculate seismograms generated by a monopole source in an elliptical borehole but did not report how the ellipticity affects the velocity dispersion. We use perturbation theory to determine the significance of the borehole irregularities upon the velocity dispersion.

METHOD

The borehole model consists of two layers — an inviscid fluid in a cylindrical borehole surrounded by a perfectly elastic, homogeneous formation (Figure 1). Each layer is characterized by its density, ρ, and elastic moduli, c_{ijkl}. The layers extend to infinity along the axis of the borehole and the outermost layer extends to infinity in the radial direction. From the entire model, only a volume element, V, having the shape of disk and a thickness of one wavelength, Λ, is needed because guided wave propagation in

every element is the same. The surface between the layers (i.e., the fluid-formation interface), which is inside the volume element, is designated Σ^i, and the surfaces at the end faces and at infinite radius, which are on the exterior of the element, Σ^e. (This two-layer model with cylindrical symmetry was chosen because it is appropriate for the geologic situations which will be studied later. Nonetheless, the equations in this section are general and can be applied to a model having many layers and any cross-sectional shape.)

Hamilton's principle will be derived for the normal modes in a borehole. Although this principle is well known, reviewing it here is necessary to show which guided waves can be studied with perturbation theory. The Lagrangian energy density is defined as the kinetic energy density minus the elastic strain energy density:

$$\mathcal{L} = \frac{1}{2}\rho \dot{u}_i \dot{u}_i - \frac{1}{2} u_{j,i} c_{ijkl} u_{l,k} \tag{1}$$

in which u_i is a displacement and $\dot{u}_i$ and $u_{l,k}$ indicate differentiation with respect to time and space. After integrating $\mathcal{L}$ over a volume element and averaging it over one period, $\mathcal{T}$, its perturbation is calculated.

$$\delta \int_t^{t+\mathcal{T}} dt \int_V dV \mathcal{L} = \int_t^{t+\mathcal{T}} dt \int_V dV \left(\rho \dot{u}_i \frac{\partial \delta u_i}{\partial t} - \delta u_{j,i} c_{ijkl} u_{l,k} \right) \tag{2}$$

Integration by parts is applied to the temporal derivatives, and Gauss' theorem transforms the volume integral with the spatial derivatives into another volume integral and two surface integrals.

$$\begin{aligned} \delta \int_t^{t+\mathcal{T}} dt \int_V dV \mathcal{L} \;=\; & \int_V dV \rho \dot{u}_i \delta u_i \,|_t^{t+\mathcal{T}} + \\ & \int_t^{t+\mathcal{T}} dt \left[- \int_V dV (\rho \ddot{u}_i - \tau_{ji,j}) \delta u_i + \int_{\Sigma^i} dS \, [n_j \tau_{ji} \delta u_i]_-^+ \right. \\ & \left. - \int_{\Sigma^e} dS n_j \tau_{ji} \delta u_i \right] \end{aligned} \tag{3}$$

The stress tensor is τ_{ji}, and the normal to a surface, n_i. The notation, $[\cdot]_-^+$, indicates the change in the quantity, $[\cdot]$, across an interface with the positive contribution from the outside surface. By convention, the perturbed displacements are chosen to be zero at t and $t+\mathcal{T}$ making the second volume integral zero. The third volume integral is zero if the displacements satisfy the equations of motion. The surface integrals account for the flux of energy through the internal and external surfaces of the volume element. The surface integral over Σ^i is zero if the stress and the perturbed displacements are periodic and satisfy the boundary conditions. The integral over Σ^e is zero if the stresses are zero at infinite radius and the net flux through the end faces is zero. These conditions are satisfied for normal modes which consist of two traveling waves (e.g.,

tube, pseudo-Rayleigh, or flexural waves) propagating in opposite directions. (Note that a normal mode cannot be constructed from two leaky P-waves because these waves radiate S-wave energy away from the center of the volume element making the surface integrals nonzero.) When Hamilton's principle is applied to a normal mode,

$$\delta \int_t^{t+\mathcal{T}} dt \int_V \mathcal{L} = 0 \quad , \tag{4}$$

which states that the time-averaged Lagrangian energy for a normal mode is stationary for perturbations in displacement which satisfy the boundary conditions. Moreover, time-averaged Lagrangian energy is zero, that is:

$$\int_t^{t+\mathcal{T}} dt \int_V \mathcal{L} = 0 \quad , \tag{5}$$

which can be derived by multiplying the equation of motion by u_i and reversing the integrations which were used to derive Hamilton's principle.

Perturbation theory will be used to relate changes in the elastic moduli, densities, locations of interfaces, frequency, and wavenumber. The mathematical formulation is similar to that used by Woodhouse and Dahlen (1978) and by Aki and Richards (1980) and is based upon an idea first proposed by Rayleigh (1945). The Lagrangian energy density is considered a function of the displacements, frequency (ω), wavenumber (W), elastic moduli, densities, and locations of interfaces (which are on Σ^i) and will be designated $\mathcal{L}(u_i, \omega, W, c_{ijkl}, \rho, \Sigma^i)$. For an appropriate model, the displacements, frequency, and wavenumber can be calculated exactly using analytical expressions. Perturbation theory is used to determine the frequency or wavenumber of another model which has slightly different elastic moduli, densities, and locations of interfaces. For this perturbed model, the Lagrangian energy density, which is expressed exactly in terms of the original model as $\mathcal{L}^p(u_i + \delta u_i, \omega + \delta\omega, W + \delta W, c_{ijkl} + \delta c_{ijkl}, \rho + \delta\rho, \Sigma^i + \delta\Sigma^i)$, is integrated over the volume element and averaged over one period.

$$\begin{aligned}
&\int_t^{t+\mathcal{T}} dt \int_V dV \mathcal{L}^p = \\
&\quad \int_t^{t+\mathcal{T}} dt \Bigg[\int_V dV \frac{1}{2}(\rho + \delta\rho)(\dot{u}_i + \delta\dot{u}_i + u_i\delta\omega)(\dot{u}_i + \delta\dot{u}_i + u_i\delta\omega) \\
&\qquad - \int_V dV \frac{1}{2}(u_{j,i} + \delta u_{j,i} + \delta_W e_{ij})(c_{ijkl} + \delta c_{ijkl})(u_{l,k} + \delta u_{l,k} + \delta_W e_{kl}) \\
&\qquad + \int_{\Sigma^i} dS \, [-h\mathcal{L}]_-^+ \Bigg]
\end{aligned} \tag{6}$$

The strain tensor is e_{ij}. The perturbations in displacement (i.e., $\delta\dot{u}_i$, δu_j, and δu_l) and frequency (i.e., $\delta\omega$) are expressed explicitly, and the perturbations in wavenumber (i.e., $\delta_W e_{ij}$ and $\delta_W e_{kl}$) implicitly. The surface integral accounts for the change in the

Lagrangian energy due to the changes in the locations of the interfaces. (The location of each perturbed interface is specified by moving the original interface a distance, h, along its normal.) The expressions in the integrands are multiplied and only terms to first order are kept. Integration by parts is applied to the temporal derivatives and Gauss' theorem to the spatial derivatives.

$$\begin{aligned}
&\int_t^{t+\mathcal{T}} dt \int_V dV \mathcal{L}^p = \\
&\quad \int_t^{t+\mathcal{T}} dt \int_V dV \left(\frac{1}{2}\rho \dot{u}_i \dot{u}_i - \frac{1}{2} u_{j,i} c_{ijkl} u_{l,k}\right) + \int_V dV \rho \dot{u}_i \delta u_i \Big|_t^{t+\mathcal{T}} \\
&\quad \int_t^{t+\mathcal{T}} dt \Bigg[- \int_V dV (\rho \ddot{u}_i - \tau_{ji,j}) \delta u_i - \int_{\Sigma^e} dS n_j \tau_{ji} \delta u_i + \int_{\Sigma^i} dS \left[n_j \tau_{ji} \delta u_i\right]_-^+ \\
&\qquad + \int_{\Sigma^i} dS \left[-h\mathcal{L}\right]_-^+ - \int_V dV \delta W e_{ij} c_{ijkl} e_{kl} + \int_V dV \rho \omega \delta \omega u_i u_i \\
&\qquad + \int_V dV \left(\frac{1}{2}\delta\rho\omega^2 u_i u_i - \frac{1}{2} e_{ij} \delta c_{ijkl} e_{kl}\right)\Bigg] \qquad (7)
\end{aligned}$$

Equations 5 shows that the first and second integrals are zero. The third, fourth, and fifth integrals are zero for the same reasons that they were zero when Hamilton's principle was applied to the normal modes. The sixth integral is not zero because the locations of the interfaces have changed. In Appendix A, its integrand is manipulated to remove the unknown, δu_i, and the result is

$$\left[n_j \tau_{ji} \delta u_i\right]_-^+ = \left[-h n_i \tau_{ij} n_k u_{j,k} + h_{,i} u_i n_j n_k \tau_{kj}\right]_-^+ \quad .$$

The first term on the right-hand side accounts for the change in the displacements between the original and the perturbed interfaces, and the second term for the change in the normal, $-h_{,i}$. With these simplifications, the final equation is

$$\begin{aligned}
&\int_t^{t+\mathcal{T}} dt \left[\int_V dV \delta W e_{ij} c_{ijkl} e_{kl} - \omega \delta\omega \int_V dV \rho u_i u_i\right] = \\
&\quad \int_t^{t+\mathcal{T}} dt \Bigg[- \int_{\Sigma^i} dS\, h \left[\mathcal{L} + n_i \tau_{ij} n_k u_{j,k}\right]_-^+ + \int_{\Sigma^i} dS\, h_{,i} \left[u_i n_j n_k \tau_{kj}\right]_-^+ \\
&\qquad + \frac{\omega^2}{2} \int_V dV \delta\rho u_i u_i - \frac{1}{2} \int_V dV e_{ij} \delta c_{ijkl} e_{kl}\Bigg] \quad . \qquad (8)
\end{aligned}$$

The first and second integrals are associated with perturbations in the wavenumber and frequency, respectively. The third integral accounts for the change in the Lagrangian energy and displacements due to the changes in the locations of the interfaces, and the fourth for the changes in the normal to each interface. The fifth and sixth integrals account for perturbations in the densities and elastic moduli, respectively.

RESULTS AND DISCUSSION

Equation 8 will be used to calculate partial derivatives, group velocity, and the effects of borehole irregularities. Because the formation is transversely isotropic (i.e., the axis of symmetry is aligned with the borehole) the elastic properties of the formation are characterized uniquely by only five elastic moduli, c_{11}, c_{13}, c_{33}, c_{44}, and c_{66}. (To derive the integrals for this borehole model, abbreviated subscript notation was used instead of tensor notation.) The elastic modulus for the fluid is the incompressibility, λ_f. The formation (which is a solid) and fluid densities are ρ_s and ρ_f, respectively.

Mathematical expressions for the displacements and strains, which are listed in Appendix B, are substituted into equation 8, and almost all of the multiple integrals are computed analytically.

$$\int_t^{t+\mathcal{T}} dt \int_V dV \delta_W e_{ij} c_{ijkl} e_{kl} = \delta l \frac{\zeta \pi \Lambda \mathcal{T}}{4} I^l \tag{9}$$

$$\int_t^{t+\mathcal{T}} dt \int_V dV \rho u_i u_i = \frac{\zeta \pi \Lambda \mathcal{T}}{4} I^\omega \tag{10}$$

$$\int_t^{t+\mathcal{T}} dt \int_{\Sigma^i} dS\, h \left[\mathcal{L} + n_i \tau_{ij} n_k u_{j,k}\right]_-^+ = \frac{\Lambda \mathcal{T}}{4} I_1^h \tag{11}$$

$$\int_t^{t+\mathcal{T}} dt \int_{\Sigma^i} dS\, h_{;i} \left[u_i n_j n_k \tau_{kj}\right]_-^+ = \frac{\Lambda \mathcal{T}}{4} I_2^h \tag{12}$$

$$\int_t^{t+\mathcal{T}} dt \int_V dV \delta \rho u_i u_i = \frac{\zeta \pi \Lambda \mathcal{T}}{4} (\delta \rho_f I_f^\rho + \delta \rho_s I_s^\rho) \tag{13}$$

$$\int_t^{t+\mathcal{T}} dt \int_V dV e_{ij} \delta c_{ijkl} e_{kl} = \frac{\zeta \pi \Lambda \mathcal{T}}{4} \left(\delta \lambda_f I_f^\lambda + \sum_{i=1}^{5} \delta c_i I_s^{c_i} \right) \tag{14}$$

The integration over time yields $\mathcal{T}/2$. The volume integrals are computed in the circular cylindrical coordinate system with coordinates r, θ, and z. The integration over axial distance yields $\Lambda/2$, and over azimuth $\zeta\pi$. When the azimuthal order number is 0, $\zeta = 2$; otherwise $\zeta = 1$. The integral over radius, which in general cannot be computed analytically, is simply given the generic designation I and is listed in Appendix C. The surface integrals involve single integrals over axial distance and azimuth which can be computed analytically for simple perturbations in the location of the fluid-formation interface. Because only perturbations in this interface with respect to azimuth are studied, the integration over axial distance yields $\Lambda/2$. The expressions for the integration over azimuth are denoted I_1^h and I_2^h and are listed in Appendix C. In equation 14 the five elastic constants for the formation are represented by c_i.

Partial Derivatives

Partial derivatives are calculated by relating perturbations in either the elastic moduli or density to perturbations in either the frequency or wavenumber. To demonstrate the procedure, the partial derivative of the wavenumber with respect to an elastic modulus of the formation will be calculated. Equations 9, 10, 11, 12, 13, and 14 are substituted into equation 8 which simplifies to the derivative,

$$\frac{\delta l}{\delta c_i} = -\frac{1}{2}\frac{I_s^{\delta c_i}}{I^{\delta l}} \quad ,$$

because the frequency, borehole shape, densities and all elastic moduli except c_i are constant. This equation is used to calculate the partial derivative of the phase velocity, v, at constant frequency with $\delta l = -l\delta v/v$. The normalized partial derivative of the phase velocity is dimensionless and is called the sensitivity,

$$\frac{c_i}{v}\frac{\delta v}{\delta c_i} = \frac{c_i}{2l}\frac{I_s^{c_i}}{I^l} \quad .$$

A sensitivity can be interpreted as the percent change in phase velocity due to a one percent change in an elastic modulus or a density. The formulas for all partial derivatives and sensitivities at constant frequency are listed in Table 1. Partial derivatives and sensitivities at constant wavenumber are calculated similarly using $\delta\omega = l\delta v$, and, for example, the sensitivity due an elastic modulus of the formation would be

$$\frac{c_i}{v}\frac{\delta v}{\delta c_i} = \frac{c_i}{2\omega^2}\frac{I_s^{c_i}}{I^l} \quad .$$

Examples of sensitivities at constant frequency for flexural waves are shown in Figure 2. The transversely isotropic formation was selected to be the Green River shale whose physical properties are tabulated by Thomsen (1986). The integration over radius was performed numerically using Gaussian quadrature and was terminated when the sum converged to four significant digits. A more extensive compilation of sensitivities in hard and soft formations is given by Ellefsen et al. (1988).

Some simple additions can be used to check the accuracy of the sensitivities. Summing those sensitivities at constant wavenumber associated with the elastic moduli gives

$$\begin{aligned} S &= \frac{\lambda_f}{2\omega^2}\frac{I_f^{\lambda}}{I^{\omega}} + \sum_{i=1}^{5}\frac{c_i}{2\omega^2}\frac{I_s^{c_i}}{I^{\omega}} \\ &= \frac{1}{2}\frac{1}{\zeta\pi\Lambda\mathcal{T}\omega^2 I^{\omega}/8}\left[\frac{\zeta\pi\Lambda\mathcal{T}}{8}\left(\lambda_f I_f^{\lambda} + \sum_{i=1}^{5} c_i I_s^{c_i}\right)\right] \quad . \end{aligned} \tag{15}$$

The expression $\zeta\pi\Lambda\mathcal{T}\omega^2 I^\omega/8$ is the time-averaged kinetic energy, and the expression within the brackets is the time-averaged elastic strain energy. Because these energies are equal (see equation 5), the sum, S, must be 1/2. Since each of the six terms in equation 15 is the fraction of the total elastic strain energy associated with an elastic modulus, the terms are frequently called partition coefficients. A similar check can be applied to the densities, and the sum must be $-1/2$. At constant frequency, the sensitivities must be multiplied by U/c (in which U is the group velocity), and the sum must be 1/2 for the elastic moduli and $-1/2$ for the densities. The computer programs, which were written to perform the calculations presented in this paper, almost always yield sums between 0.4999 and 0.5001, and higher accuracy could easily be obtained.

When the formation is isotropic, the partial derivatives can be readily calculated with the previous equations. Using the Lamé parameters, which are related to the general elastic moduli via $c_{11} = c_{33} = \lambda_s + 2\mu_s$, $c_{13} = \lambda_s$, and $c_{44} = c_{66} = \mu_s$, equation 14 may be written

$$\int_t^{t+\mathcal{T}} dt \int_V dV e_{ij}\delta c_{ijkl} e_{kl} = \frac{\zeta\pi\Lambda\mathcal{T}}{4} \times \left[\delta\lambda_f I_f^\lambda + \delta(\lambda_s + 2\mu_s)(I_s^{c11} + I_s^{c33} + I_s^{c13}) + \delta\mu_s(I_s^{c44} + I_s^{c66} - 2I_s^{c13})\right] \tag{16}$$

Partial derivatives of the wavenumber and frequency are calculated by substituting this expression into equation 8. Usually the derivative with respect to the formation P- or S-wave velocity (α_s and β_s, respectively) is desired and can be obtained with $2(\lambda_s+2\mu_s)/\delta(\lambda_s+2\mu_s) = \alpha_s/\delta\alpha_s$ and $2\mu_s/\delta\mu_s = \beta_s/\delta\beta_s$. Similarly the derivative with respect to the fluid acoustic velocity is found with $2\lambda_f/\delta\lambda_f = alpha_f/\delta\alpha_f$. (The 2 in these equations causes the sensitivities to sum to 1.) Table 2 lists partial derivatives and sensitivities at constant frequency. Partial derivatives and sensitivities at constant wavenumber are derived in a similar manner.

Group Velocity

Group velocity is calculated by relating perturbations in frequency and wavenumber. Equation 8 reduces to

$$U = \frac{\delta\omega}{\delta l} = \frac{1}{\omega}\frac{I^l}{I^\omega} \tag{17}$$

because the borehole shape, densities, and elastic moduli are constant. Examples of group velocities for the tube and flexural waves in a transversely isotropic formation are shown in Figure 3, and additional examples are given by Ellefsen et al. (1988).

Slightly Irregular Borehole

Three steps are required to calculate the phase velocities of guided waves in irregular boreholes. First, dispersion curves are calculated for a circular cylindrical borehole for which the radius is close to the average radius of the irregular borehole. Second, the perturbations in wavenumber due to the irregular borehole wall are calculated with equation 8. Assuming that the frequency is constant and using $\delta l = -l\delta v/v$, perturbations in wavenumber can be related to perturbations in phase velocity:

$$\delta v = \frac{\omega}{\zeta \pi l^2} \frac{I_1^h - I_2^h}{I^l} \quad . \tag{18}$$

Third, these velocity corrections are added to the original dispersion curves. However, because the corrections are usually small, comparing the dispersion curves for the circular and irregular boreholes would not be worthwhile. Instead the corrections are displayed as the percent change in the phase velocity, $100\% \times \delta v/v$.

Test results show that the estimated phase velocities are fairly accurate even for moderately large perturbations in the borehole wall. For the test, the formation was chosen to be isotropic and have velocities and density like those for the Berea sandstone. Exact dispersion curves were computed for two cylindrical boreholes (Figure 4a) with radii, R and $R+\epsilon R$, for which R was 0.1016 m (4.0 in.) and ϵ a scaling parameter. The difference between the velocities at each frequency is the exact perturbation, which is shown in Figure 4b for the tube wave. Equation 8 was used to estimate the same perturbations by changing the location of the borehole wall with $h(\theta) = \epsilon R$, and the results are shown in Figure 4b. For small changes in radius, the velocity perturbations are very accurate, but as the changes increase, the perturbations become biased at moderate and high frequencies. This discrepancy between the exact and estimated velocity perturbations is also observed with the other guided waves. Based upon these results, the maximum change in borehole shape, for which equation 8 could give reasonably accurate velocity perturbations, was assumed to be 10% of the radius (i.e., $\epsilon = 0.10$).

Velocity perturbations were calculated for three irregular boreholes which are common in field situations (R. Siegfried, 1988, personal communication). The irregularities only depend upon azimuth; irregularities with respect to z were not considered because the rough borehole would cause scattering (see e.g., Brekhovskikh, 1959 or Bouchon and Schmitt, 1989). The scaling parameter, ϵ, was chosen to be 0.10. The formation properties are like those for the Berea sandstone, and the borehole radius is 0.1016 m. The first example is an elliptically-shaped borehole (Figure 5a), which was created by perturbing the cylindrical borehole wall with $h(\theta) = R\epsilon \cos^2(\theta - \phi)$. The angle, ϕ, is the orientation of the long axis of the perturbation in the borehole wall relative to the reference axis for the circular cylindrical coordinate system. The percent change in the phase velocity as a function of frequency is displayed in Figures 5b and 5c. The

second example is an egg-shaped borehole (Figure 6a), for which

$$h(\theta) = \begin{cases} R\epsilon \cos^2(\theta - \phi) & \text{for } -\frac{\pi}{2} \le \theta - \phi \le \frac{\pi}{2} \\ 0 & \text{for } \frac{\pi}{2} < \theta - \phi < \frac{3\pi}{2} \end{cases} ,$$

and the changes in velocity are shown in Figures 6b and 6c. The velocity changes for this egg-shaped borehole are exactly half those for the elliptical borehole, because the irregularity is exactly the same over half of the borehole wall. The third example is a borehole with three lobes (Figure 7a) for which $h(\theta) = R\epsilon \cos^2 \frac{3}{2}(\theta - \phi)$, and the velocity changes are shown in Figure 7b. Because h is directly proportional to ϵ in all three examples, the calculated velocity changes can be used to estimate velocity changes for similar situations by direct scaling.

The changes in the velocities depend upon the basic properties of the guided waves. The changes for the pseudo-Rayleigh, flexural, and screw waves waves are always negative because the increase in the average borehole radius has shifted the dispersion curves to lower frequencies. The magnitude of the changes are very large near the Airy phase. To understand this phenomenon, these waves may be considered a hybridization of surface and multiply-reflected waves (Paillet and White, 1982; Schmitt and Bouchon, 1985). The perturbations in the borehole shape affect the constructive and destructive interference of the multiply-reflected part of these waves and consequently alter the phase velocity. Near the cutoff frequency, the magnitude of the change is very small because the phase velocity of a normal mode in the irregular borehole cannot exceed the formation S-wave velocity, as it cannot in a circular borehole (Biot, 1952). The velocity changes here are not zero due to the shift in the dispersion curve. At high frequencies, the magnitude of the change approaches zero because the fluid-formation interface appears planar to the guided wave as it does in a circular borehole. The changes for the tube wave are always positive because the average borehole radius has increased (c.f., the test example). As the frequency approaches zero, the changes also approach zero because the velocity at zero frequency does not depend upon the radius (White, 1983). The velocity changes for the tube wave are relatively small because it is a Stoneley wave which does not contain a multiply-reflected part.

The cross-sectional shape of the borehole and the azimuthal order number of the guided wave (n) are important factors in the velocity perturbations. The velocity changes for the tube and pseudo-Rayleigh wave are never affected by the orientation of the borehole irregularity, but the velocity changes for the flexural wave are. For the elliptical and egg-shaped boreholes, the largest correction occurs when the long axis of the irregularity is aligned with the flexural wave, and smallest when it is perpendicular to the wave. Equations 11 and 12 express the physics of this behavior. In equation 11, h is averaged over θ with weights, $\cos^2 n\theta$ and $\sin^2 n\theta$, and in equation 12 $dh/d\theta$ is averaged over θ with weight, $\cos 2n\theta$. The tube and pseudo-Rayleigh waves (for which $n = 0$) smooth h and $dh/d\theta$ completely, and consequently their velocity perturbations are independent of the orientation of the perturbation. The flexural and screw waves

(for which $n = 1$ and $n = 2$, respectively) can have very large or small averages depending upon the orientation of the perturbation and its mathematical expression.

The effect of an irregular borehole upon the velocity dispersion is insignificant for many field situations. In the examples presented here, the velocity perturbations for the tube wave were always less than $\frac{1}{2}\%$, and for the other guided waves generally about 5%. Similar results were obtained for boreholes with radii of 0.0762 m (3.0 in) and 0.127 m (5.0 in). Although ϵ was chosen to 0.10 for these examples, it is usually less than about 0.03 or 0.04 for most field situations (R. Siegfried, 1988, personal communication). By direct scaling, the expected perturbations would be almost zero for the tube wave and less than about 2% for the other guided waves. Velocity perturbations of this size are difficult to detect.

CONCLUSIONS

First order perturbation theory with Hamilton's principle has been applied to guided wave propagation in a borehole. The formation was assumed to be perfectly elastic, and the fluid inviscid. With this method, perturbations in frequency, wavenumber, elastic moduli, density, and the locations of interfaces can be related. Because Hamilton's principle only applies to normal modes, only waves like the tube, pseudo-Rayleigh, and flexural waves can be studied.

Using a model with two layers, relations between the perturbations were used to address three problems in acoustic logging. (1) A method for calculating the partial derivative of the wavenumber or frequency with respect to an elastic modulus or density was presented. Normalizing the partial derivatives gives the sensitivities of the phase velocity with respect to an elastic modulus or density, and the accuracy of the sensitivities can be checked with some simple additions. The equations for the partial derivatives and sensitivities for isotropic formations are only a slight modification of those equations for the transversely isotropic formation. (2) A method of calculating the group velocity of a guided wave in a transversely isotropic formation was presented. (3) A method of calculating changes in the phase velocity of a guided wave due to irregularities in the cross-sectional shape of the borehole was presented.

The effect which three common borehole shapes (i.e., elliptical, egg-shaped, and three-lobed) have on the velocities was calculated. Although the velocity perturbations for each shape and for each guided wave are different, several generalization can be made. The tube and pseudo-Rayleigh waves completely smooth the effects of the irregularity making the velocity perturbations independent of the wave's orientation with respect to the irregularity. The perturbations for the tube wave are very small because it is a Stoneley wave, but those for the pseudo-Rayleigh wave are much larger because the irregularities affect the multiply-reflected part of this wave. The pertur-

bations are largest near the Airy phase and are quite small near the cutoff frequency and at high frequencies. The velocity perturbations for the flexural and screw waves are similar in character to those for the pseudo-Rayleigh wave. However, because these waves are directional, they can sometimes interact with the borehole irregularity which can amplify or diminish the perturbation. The effect of moderately-sized borehole irregularities is probably insignificant for most field situations.

ACKNOWLEDGEMENTS

This work was supported by the Full Waveform Acoustic Logging Consortium at MIT. K. J. Ellefsen is partially supported by the Phillips Petroleum Fellowship.

REFERENCES

Aki, K. and P. G. Richards, *Quantitative Seismology,* W. H. Freeman & Co., 1980.

Biot, M. A., Propagation of elastic waves in cylindrical bore containing a fluid, *J. Appl. Phys., 23,* 997–1005, 1952.

Bouchon, M. and D. P. Schmitt, Full wave logging in an irregular borehole, 1989, submitted to *Geophysics.*

Brekhovskikh, L. M:, Propagation of surface Rayleigh waves along the uneven boundary of an elastic body, *Soviet Phys. Acoust., 5,* 288–295, 1959.

Burns, D. R. and C. H. Cheng, Inversion of borehole guided wave amplitudes for formation shear wave attenuation values, *J. Geophys. Res., 92,* 12713–12725, 1987.

Cheng, C. H., M. N. Toksöz, and M. E. Willis, Determination of in situ attenuation from full waveform acoustic logs, *J. Geophys. Res., 87,* 5477–5484, 1982.

Dahlen, F. A., Reply, *J. Geophys. Res., 81,* 4951–4956, 1976.

Ellefsen, K. J., C. H. Cheng, and D. P. Schmitt, Acoustic logging guided waves in transversely isotropic formations, in *Trans., SPWLA, 29th Ann. Logging Symp.,* 1988, paper YY.

Paillet, F. L. and J. E. White, Acoustic modes of propagation in the borehole and their relationship to rock properties, *Geophysics, 47,* 1215–1228, 1982.

Rayleigh, J. W. S., *The Theory of Sound,* vol. 1, Dover Publ. Inc., 1945.

Schmitt, D. P. and M. Bouchon, Full-wave acoustic logging: synthetic microseismograms and frequency-wavenumber analysis, *Geophysics, 50,* 1756–1778, 1985.

Smith, M. L., The scalar equations of infinitesimal elastic-gravitational motion for a rotating, slightly elliptical Earth, *Geophys. J. Roy. Astron. Soc., 37,* 491–526, 1973.

Stevens, J. L. and S. M. Day, Shear velocity logging in slow formations using the Stoneley wave, *Geophysics, 51,* 137–147, 1986.

Thomsen, L., Weak elastic anisotropy, *Geophysics, 51,* 1954–1966, 1986.

Toksöz, M. N., C. H. Cheng, and M. E. Willis, Seismic waves in a borehole — A review, in *Vertical Seismic Profiling, Part B: Advanced Concepts,* edited by M. N. Toksöz and R. R. Stewart, pp. 256–275, Geophysical Press, 1984.

Tongtaow, C., *Wave propagation along a cylindrical borehole in a transversely isotropic formation,* Ph.D. thesis, Colorado School of Mines, Golden, CO, 1982.

White, J. E., *Underground Sound,* Elsevier Science Publ. Co., Inc., 1983.

Willen, D. E., A perturbative approach to sonic logging in a borehole, in *53th Ann. Internat. Mtg., Soc. Expl. Geophys., Expd. Abst.,* pp. 1–2, Las Vegas, NV, 1983.

Winterstein, D. F., Anisotropy effects in P-wave and SH-wave stacking velocities contain information on lithology, *Geophysics, 51,* 661–672, 1986.

Woodhouse, J. H. and F. A. Dahlen, The effect of a general aspherical perturbation on the free oscillations of the Earth, *Geophys. J. Roy. Astron. Soc., 53,* 335–354, 1978.

Zoback, M. D., State of stress in the lithosphere, *Rev. Geophys. Space Phys., 21,* 1503–1511, 1983.

APPENDIX A

In this appendix, the integrand, $[n_j \tau_{ji} \delta u_i]_-^+$, which appears in equation 7, will be manipulated to remove the unknown, δu_i. Woodhouse and Dahlen (1978) present the result without any derivation. We will give the derivation using some of the equations which appear in Dahlen (1976) and Smith (1974).

The boundary conditions on the perturbed interfaces will be expressed in terms of the boundary conditions on the unperturbed interfaces. On a perturbed, welded interface (i.e., a solid-solid interface) the displacements are continuous:

$$[u_i + \delta u_i + h n_k u_{i,k}]_-^+ = 0 \quad . \qquad (A-1)$$

The second term is the perturbation in the displacement due to the perturbed interface, and the third term is a linear extrapolation of the original displacement from the original to the perturbed interface. Because $[u_i]_-^+ = 0$,

$$[\delta u_i]_-^+ = [-h n_k u_{i,k}]_-^+ \quad . \qquad (A-2)$$

On a perturbed, frictionless interface (i.e., a fluid-solid interface) the normal component of displacement is continuous:

$$[(n_i - h_{;i})(u_i + \delta u_i + h n_k u_{i,k})]_-^+ = 0 \quad . \qquad (A-3)$$

The term, $-h_{;i}$, is the change in the normal between the perturbed and unperturbed interfaces, and $h_{;i} = h_{,i} - n_i(n_j h_{,j})$. To first order, this equation is

$$[n_i \delta u_i]_-^+ = [-h n_i n_k u_{i,k} + h_{;i} u_i]_-^+ \qquad (A-4)$$

because $[n_i u_i]_-^+ = 0$. On all perturbed interfaces the traction is continuous:

$$[(n_i - h_{;i})(\tau_{ij} + \delta \tau_{ij} + h n_k \tau_{ij,k})]_-^+ = 0 \quad . \qquad (A-5)$$

The second term in the expression for the stress, $\delta \tau_{ij}$, is the perturbation in the stress due to the perturbed interface, and the third term is a linear extrapolation of the original stress from the original to the perturbed interface. To first order, this equation is

$$[n_i \delta \tau_{ij}]_-^+ = [-h n_i n_k \tau_{ij,k} + h_{;i} \tau_{ij}]_-^+ \quad . \qquad (A-6)$$

because $[n_i \tau_{ij}]_-^+ = 0$.

These boundary conditions will now be used to derive an expression for $[n_j \tau_{ji} \delta u_i]_-^+$. On a welded interface, equation A-2 may be directly substituted into $[n_j \tau_{ji} \delta u_i]_-^+$:

$$[n_j \tau_{ji} \delta u_i]_-^+ = [-h n_j \tau_{ji} n_k u_{i,k}]_-^+ \quad . \qquad (A-7)$$

The traction, T_i, will be used to simplify the derivation for a frictionless interface. Because the traction is normal to the interface,

$$[T_i \delta u_i]_-^+ = [n_j T_j n_i \delta u_i]_-^+ \quad . \qquad (A-8)$$

Equation A-4 is substituted into the previous equation:

$$[T_i \delta u_i]_-^+ = [-h T_i n_k u_{i,k} + h_{;i} u_i n_j T_j]_-^+ \quad , \qquad (A-9)$$

and the traction is replaced by the normal component of the stress:

$$[n_j \tau_{ji} \delta u_i]_-^+ = [-h n_j \tau_{ji} n_k u_{i,k} + h_{;i} u_i n_j n_k \tau_{kj}]_-^+ \quad . \qquad (A-10)$$

On a welded interface, this equation would reduce to equation A-7 because the last term would be zero. Therefore, equation A-10 holds for all interfaces.

APPENDIX B

The equations for the displacements associated with a normal mode in a fluid-filled borehole through a transversely isotropic formation are presented in this appendix. These equations are based upon the expressions which Tongtaow (1982) derived for a travelling wave in a borehole with a tool.

The displacements have this general form:

$$\begin{aligned} u_r(r,\theta,z,t) &= \frac{1}{2}\left[U_r(r)e^{ilz} + U_r^*(r)e^{-ilz}\right]\cos(n\theta)\cos(\omega t) \\ u_\theta(r,\theta,z,t) &= \frac{1}{2}\left[U_\theta(r)e^{ilz} + U_\theta^*(r)e^{-ilz}\right]\sin(n\theta)\cos(\omega t) \\ u_z(r,\theta,z,t) &= \frac{1}{2}\left[U_z(r)e^{ilz} + U_z^*(r)e^{-ilz}\right]\cos(n\theta)\cos(\omega t) \quad . \end{aligned} \qquad (B\text{-}1)$$

In the circular cylindrical coordinate system, r is the radial distance, z the axial distance, and θ the azimuth. The axial wavenumber is l, the azimuthal order number n, and the radian frequency ω. The functions for the radial dependence of the displacements in the fluid are

$$\begin{aligned} U_r(r) &= A_1 m_1 \left[\frac{n}{m_1 r} I_n(m_1 r) + I_{n+1}(m_1 r)\right] \\ U_\theta(r) &= -\frac{A_1 n}{r} I_n(m_1 r) \\ U_z(r) &= A_1 i l I_n(m_1 r) \quad , \end{aligned} \qquad (B\text{-}2)$$

and in the formation are

$$U_r(r) = -A_2 m_2 (1 + ila') \left[-\frac{n}{m_2 r} K_n(m_2 r) + K_{n+1}(m_2 r)\right] +$$

$$\frac{C_2 n}{r} K_n(\bar{k}_2 r) - B_2 k_2 (il + b') \left[-\frac{n}{k_2 r} K_n(k_2 r) + K_{n+1}(k_2 r) \right]$$

$$U_\theta(r) = -\frac{A_2 n}{r}(1 + ila') K_n(m_2 r) + C_2 \bar{k}_2 \left[-\frac{n}{\bar{k}_2 r} K_n(\bar{k}_2 r) + K_{n+1}(\bar{k}_2 r) \right] -$$

$$\frac{B_2 n}{r}(il + b') K_n(k_2 r)$$

$$U_z(r) = A_2(il - a' m_2^2) K_n(m_2 r) - B_2(k_2^2 - ilb') K_n(k_2 r) \qquad \text{(B-3)}$$

The coefficients, A_1, A_2, B_2, and C_2, and the axial wavenumber are found by solving the period equation. Formulas for the wavenumbers, m_1, m_2, k_2, and $\bar{k}_2$, and the coupling coefficients, a' and b', are given by Tongtaow (1982).

APPENDIX C

Expressions for the integrals in equation 8, appropriate for a fluid-filled borehole through a transversely isotropic formation, are presented in this appendix.

The strains are found by differentiating the displacements listed in Appendix B, and their radial parts are designated E_{rr}, $E_{\theta\theta}$, E_{zz}, $E_{z\theta}$, E_{rz}, and $E_{r\theta}$. The displacements and strains are substituted into the integrals in equation 8, and almost all of the integrals are computed analytically. In the final expressions for the integrals ζ is 2 when $n = 0$; otherwise ζ is 1. When $n = 0$, all displacements and strains containing $\sin(n\theta)$ cancel. Because the radial dependence of these particular displacements and strains are also zero when $n = 0$, they may be included in the integrals eliminating the need to write the equations twice.

The integral associated with a perturbation in wavenumber is

$$\int_t^{t+\mathcal{T}} dt \int_V dV \delta_W e_{ji} c_{ijkl} e_{lk} = \delta l \frac{\zeta \pi \Lambda \mathcal{T}}{4} \times \qquad \text{(C-1)}$$

$$\left(\int_0^R dr\, r \lambda_f \Big[|E_{rr}||iU_z| \cos(\arg E_{rr} - \arg(iU_z)) + \right.$$

$$|E_{\theta\theta}||iU_z| \cos(\arg E_{\theta\theta} - \arg(iU_z)) + |E_{zz}||iU_z| \cos(\arg E_{zz} - \arg(iU_z)) \Big] +$$

$$\int_R^\infty dr\, r \Big\{ c_{13} \Big[|E_{rr}||iU_z| \cos(\arg E_{rr} - \arg(iU_z)) +$$

$$|E_{\theta\theta}||iU_z| \cos(\arg E_{\theta\theta} - \arg(iU_z)) \Big] + c_{33} \Big[|E_{zz}||iU_z| \cos(\arg E_{zz} - \arg(iU_z)) \Big] +$$

$$c_{44} \Big[4|E_{z\theta}||\frac{iU_\theta}{2}| \cos(\arg E_{z\theta} - \arg(\frac{iU_\theta}{2})) +$$

$$\left. 4|E_{rz}|\frac{iU_r}{2}|| \cos(\arg E_{rz} - \arg(\frac{iU_r}{2})) \Big] \Big\} \right) \quad ,$$

in which R is the borehole radius. The sum of the two integrals over radius will be designated I^l.

The integral associated with a perturbation in frequency is

$$\int_t^{t+\mathcal{T}} dt \int_V dV \rho u_i u_i = \frac{\zeta \pi \Lambda \mathcal{T}}{4} \int_0^\infty dr\, r\rho \left(|U_r|^2 + |U_\theta|^2 + |U_z|^2 \right) \quad , \qquad (C-2)$$

for which the integral over radius is designated I^ω.

Two integrals are associated with perturbations in the boundary locations. To write these two integrals, this notation will be helpful:

$$I_{cc} = \int_0^{2\pi} d\theta \cos^2(n\theta) h \qquad (C\text{-}3)$$

$$I_{ss} = \int_0^{2\pi} d\theta \sin^2(n\theta) h \qquad (C\text{-}4)$$

$$I_{cs} = \int_0^{2\pi} d\theta \cos(n\theta) \sin(n\theta) \frac{dh}{d\theta} \quad , \qquad (C\text{-}5)$$

in which h is only a function of azimuth. The first integral is

$$\int_t^{t+\mathcal{T}} dt \int_{\Sigma^i} dS\, h \left[\mathcal{L} + n_i \tau_{ij} n_k u_{j,k} \right]_-^+ = \frac{\Lambda \mathcal{T}}{4} \times \qquad (C\text{-}6)$$

$$\left[\frac{1}{2} R \left\{ \rho\omega^2 \left(|U_r(R)|^2 I_{cc} + |U_\theta(R)|^2 I_{ss} + |U_z(R)|^2 I_{cc} \right) \right\} \right.$$

$$-\frac{1}{2} R \left\{ c_{11} \left[|E_{rr}(R)|^2 + |E_{\theta\theta}(R)|^2 + \right. \right.$$

$$2|E_{rr}(R)||E_{\theta\theta}(R)| \cos(\arg E_{rr}(R) - \arg E_{\theta\theta}(R)) \Big] I_{cc} +$$

$$c_{13} \Big[2|E_{rr}(R)||E_{zz}(R)| \cos(\arg E_{rr}(R) - \arg E_{zz}(R)) +$$

$$2|E_{\theta\theta}(R)||E_{zz}(R)| \cos(E_{\theta\theta}(R) - \arg E_{zz}(R)) \Big] I_{cc} +$$

$$c_{33} \left[|E_{zz}(R)|^2 \right] I_{cc} + c_{44} \left[4|E_{z\theta}(R)|^2 I_{ss} + 4|E_{rz}(R)|^2 I_{cc} \right] +$$

$$c_{66} \left[4|E_{r\theta}(R)|^2 I_{ss} - 4|E_{rr}||E_{\theta\theta}(R)| \cos(\arg E_{rr}(R) - \arg E_{\theta\theta}(R)) I_{cc} \right] \Big\}$$

$$+R \left\{ c_{11} \left[|E_{rr}(R)|^2 + |E_{rr}(R)||E_{\theta\theta}(R)| \cos(\arg E_{rr}(R) - \arg E_{\theta\theta}(R)) \right] I_{cc} + \right.$$

$$c_{13} \left[|E_{rr}(R)||E_{zz}(R)| \cos(\arg E_{rr}(R) - \arg E_{zz}(R)) \right] I_{cc} +$$

$$\left. \left. c_{66} \left[-2|E_{rr}(R)||E_{\theta\theta}(R)| \cos(\arg E_{rr}(R) - \arg E_{\theta\theta}(R)) \right] I_{cc} \right\} \right]_-^+ \quad ,$$

and the expression delimited by the brackets, $[\cdot]_-^+$, is designated I_1^h. The second integral

is

$$\int_t^{t+\mathcal{T}} dt \int_{\Sigma^i} dS\, h_{;i} \Big[u_i n_j n_k \tau_{kj}\Big]_-^+ = \frac{\Lambda \mathcal{T}}{4} \times \tag{C-7}$$
$$\Bigg[I_{cs} \Big\{ c_{11} \Big[|E_{rr}(R)||U_\theta(R)| \cos(\arg E_{rr}(R) - \arg U_\theta(R))$$
$$+ |E_{\theta\theta}(R)||U_\theta(R)| \cos(\arg E_{\theta\theta}(R) - \arg U_\theta(R)) \Big] +$$
$$c_{13} \Big[|E_{zz}(R)||U_\theta(R)| \cos(\arg E_{zz}(R) - \arg U_\theta(R)) \Big] +$$
$$c_{66} \Big[-2|E_{\theta\theta}(R)||U_\theta(R)| \cos(\arg E_{\theta\theta}(R) - \arg U_\theta(R)) \Big] \Big\} \Bigg]_-^+ ,$$

and the expression delimited by the brackets, $[\cdot]_-^+$, is designated I_2^h.

The integrals associated with perturbations in either the fluid or formation density are

$$\int_t^{t+\mathcal{T}} dt \int_V dV\, \delta\rho u_i u_i = \frac{\zeta \pi \Lambda \mathcal{T}}{4} \times \tag{C-8}$$
$$\Big[\delta\rho_f \int_0^R dr\, r \left(|U_r|^2 + |U_\theta|^2 + |U_z|^2 \right) + \delta\rho_s \int_R^\infty dr\, r \left(|U_r|^2 + |U_\theta|^2 + |U_z|^2 \right) \Big] .$$

The integrals over radius are I_f^ρ and I_s^ρ.

The integral associated with perturbations in the elastic moduli of the fluid and transversely isotropic formation is

$$\int_t^{t+\mathcal{T}} dt \int_V dV\, e_{ji} \delta c_{ijkl} e_{lk} = \frac{\zeta \pi \Lambda \mathcal{T}}{4} \times \tag{C-9}$$
$$\Bigg(\int_0^R dr\, r \delta\lambda_f \Big[|E_{rr}|^2 + |E_{\theta\theta}|^2 + |E_{zz}|^2 + 2|E_{rr}||E_{\theta\theta}| \cos(\arg E_{rr} - \arg E_{\theta\theta}) +$$
$$2|E_{rr}||E_{zz}| \cos(\arg E_{rr} - \arg E_{zz}) + 2|E_{\theta\theta}||E_{zz}| \cos(\arg E_{\theta\theta} - \arg E_{zz}) \Big] +$$
$$\int_R^\infty dr\, r \Big\{ \delta c_{11} \Big[|E_{rr}|^2 + |E_{\theta\theta}|^2 + 2|E_{rr}||E_{\theta\theta}| \cos(\arg E_{rr} - \arg E_{\theta\theta}) \Big] +$$
$$\delta c_{13} \Big[2|E_{rr}||E_{zz}| \cos(\arg E_{rr} - \arg E_{zz}) + 2|E_{\theta\theta}||E_{zz}| \cos(\arg E_{\theta\theta} - \arg E_{zz}) \Big] +$$
$$\delta c_{33} \Big[|E_{zz}|^2 \Big] + \delta c_{44} \Big[4|E_{z\theta}|^2 + 4|E_{rz}|^2 \Big] +$$
$$\delta c_{66} \Big[4|E_{r\theta}|^2 - 4|E_{rr}||E_{\theta\theta}| \cos(\arg E_{rr} - \arg E_{\theta\theta}) \Big] \Big\} \Bigg)$$

The integrals over radius are I_f^λ and $I_s^{c_i}$ for $i = 1, \ldots, 5$.

Quantity	Partial Derivative of Wavenumber	Sensitivity
fluid density	$\frac{\delta l}{\delta \rho_f} = \frac{\omega^2}{2}\frac{I_f^\rho}{I^l}$	$\frac{\rho_f}{v}\frac{\delta v}{\delta \rho_f} = -\frac{\rho_f \omega v}{2}\frac{I_f^\rho}{I^l}$
formation density	$\frac{\delta l}{\delta \rho_s} = \frac{\omega^2}{2}\frac{I_s^\rho}{I^l}$	$\frac{\rho_s}{v}\frac{\delta v}{\delta \rho_s} = -\frac{\rho_s \omega v}{2}\frac{I_s^\rho}{I^l}$
fluid elastic modulus	$\frac{\delta l}{\delta \lambda_f} = -\frac{1}{2}\frac{I_f^\lambda}{I^l}$	$\frac{\lambda_f}{v}\frac{\delta v}{\delta \lambda_f} = \frac{\lambda_f}{2l}\frac{I_f^\lambda}{I^l}$
formation elastic modulus	$\frac{\delta l}{\delta c_i} = -\frac{1}{2}\frac{I_s^{c_i}}{I^l}$	$\frac{c_i}{v}\frac{\delta v}{\delta c_i} = \frac{c_i}{2l}\frac{I_s^{c_i}}{I^l}$

Table 1: Partial derivatives and sensitivities at constant frequency for guided waves in a fluid-filled borehole through a transversely isotropic formation.

Quantity	Partial Derivative of Wavenumber	Sensitivity
α_f	$\frac{\delta l}{\delta \alpha_f} = -\frac{\lambda_f}{\alpha_f}\frac{I_f^\lambda}{I^l}$	$\frac{\alpha_f}{v}\frac{\delta v}{\delta \alpha_f} = \frac{\lambda_f}{l}\frac{I_f^\lambda}{I^l}$
α_s	$\frac{\delta l}{\delta \alpha_s} = -\frac{\lambda_s + 2\mu_s}{\alpha_s}\frac{I_s^{c11} + I_s^{c33} + I_s^{c13}}{I^l}$	$\frac{\alpha_s}{v}\frac{\delta v}{\delta \alpha_s} = \frac{\lambda_s + 2\mu_s}{l}\frac{I_s^{c11} + I_s^{c33} + I_s^{c13}}{I^l}$
β_s	$\frac{\delta l}{\delta \beta_s} = -\frac{\mu_s}{\beta_s}\frac{I_s^{c44} + I_s^{c66} - 2I_s^{c13}}{I^l}$	$\frac{\beta_s}{v}\frac{\delta v}{\delta \beta_s} = \frac{\mu_s}{l}\frac{I_s^{c44} + I_s^{c66} - 2I_s^{c13}}{I^l}$

Table 2: Partial derivatives and sensitivities at constant frequency for guided waves in a fluid-filled borehole through an isotropic formation.

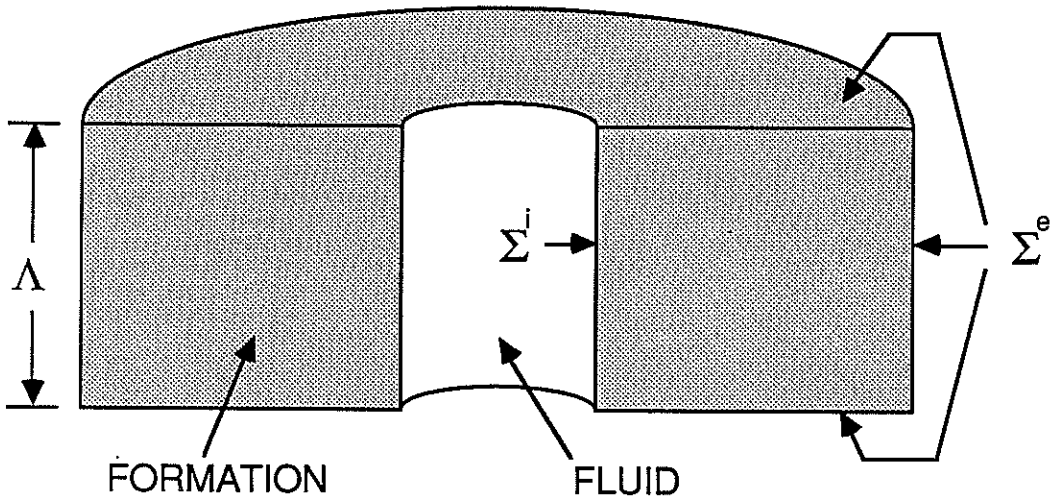

Figure 1: Cutaway view of one volume element from the borehole model. The element actually extends to infinity in the radial direction.

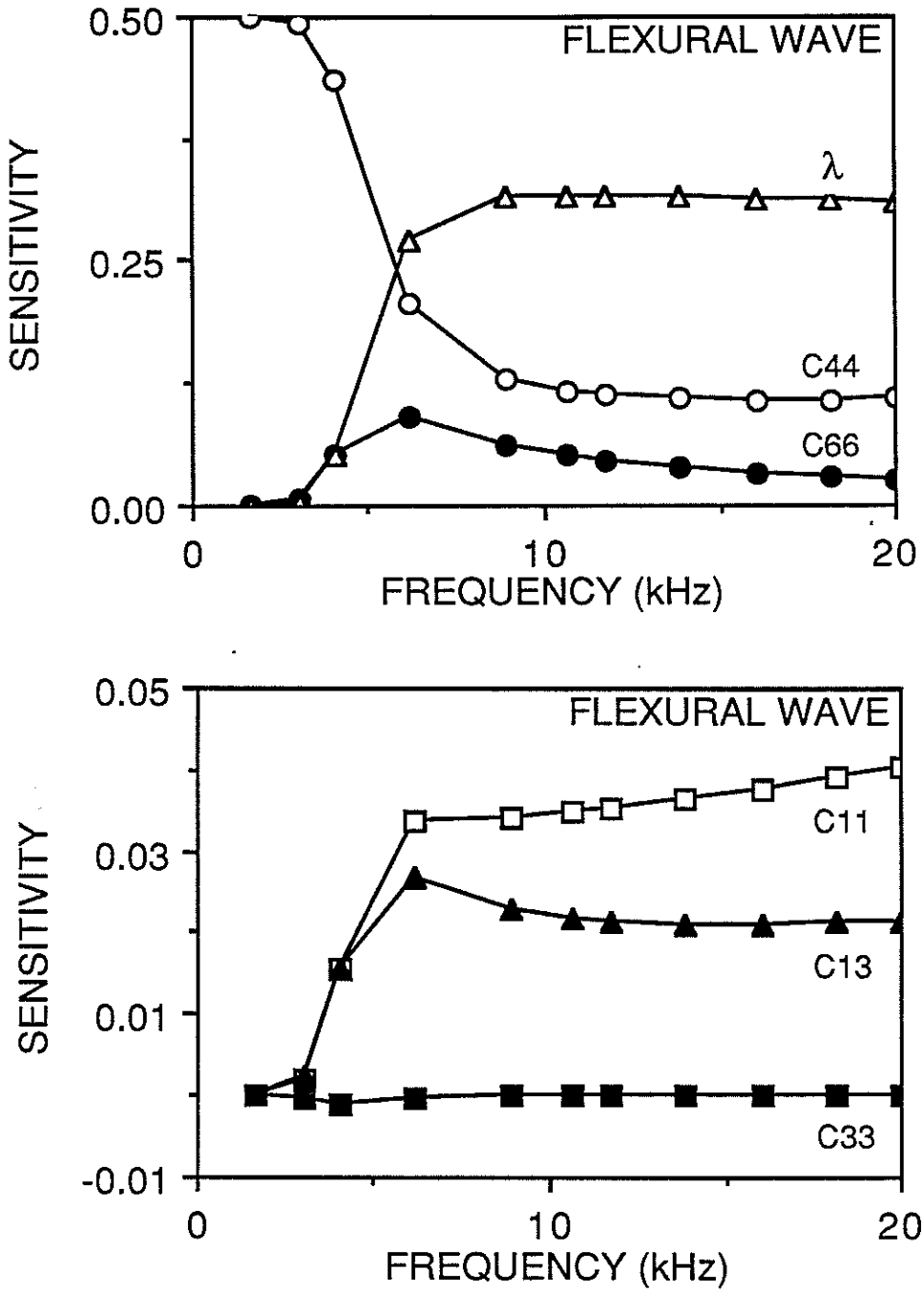

Figure 2: Velocity sensitivities at constant frequency for a flexural wave in the Green River shale.

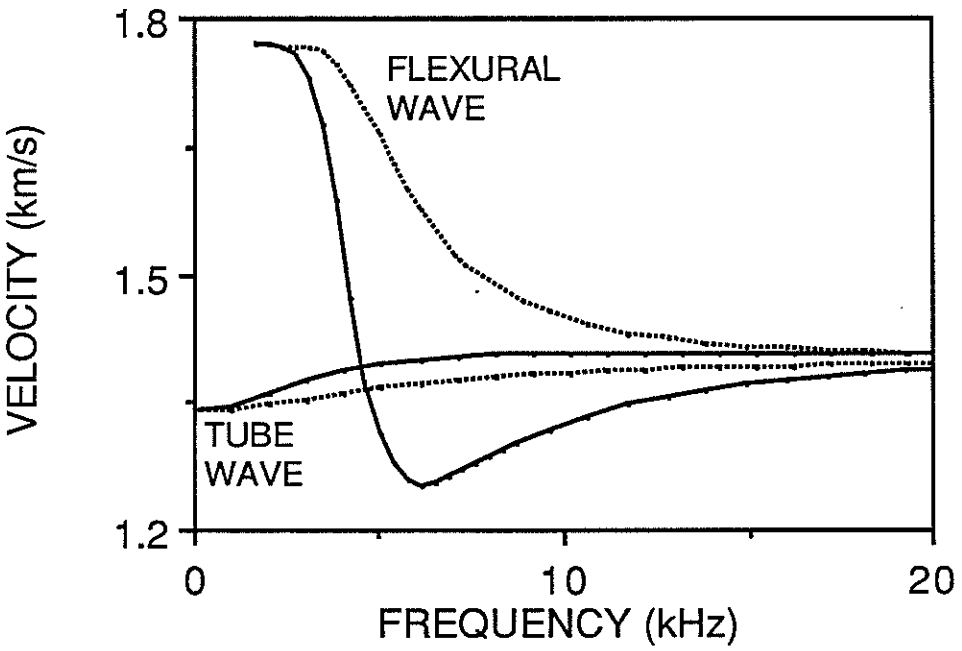

Figure 3: Phase and group velocities (dotted and solid lines, respectively) for tube and flexural waves in the Green River shale.

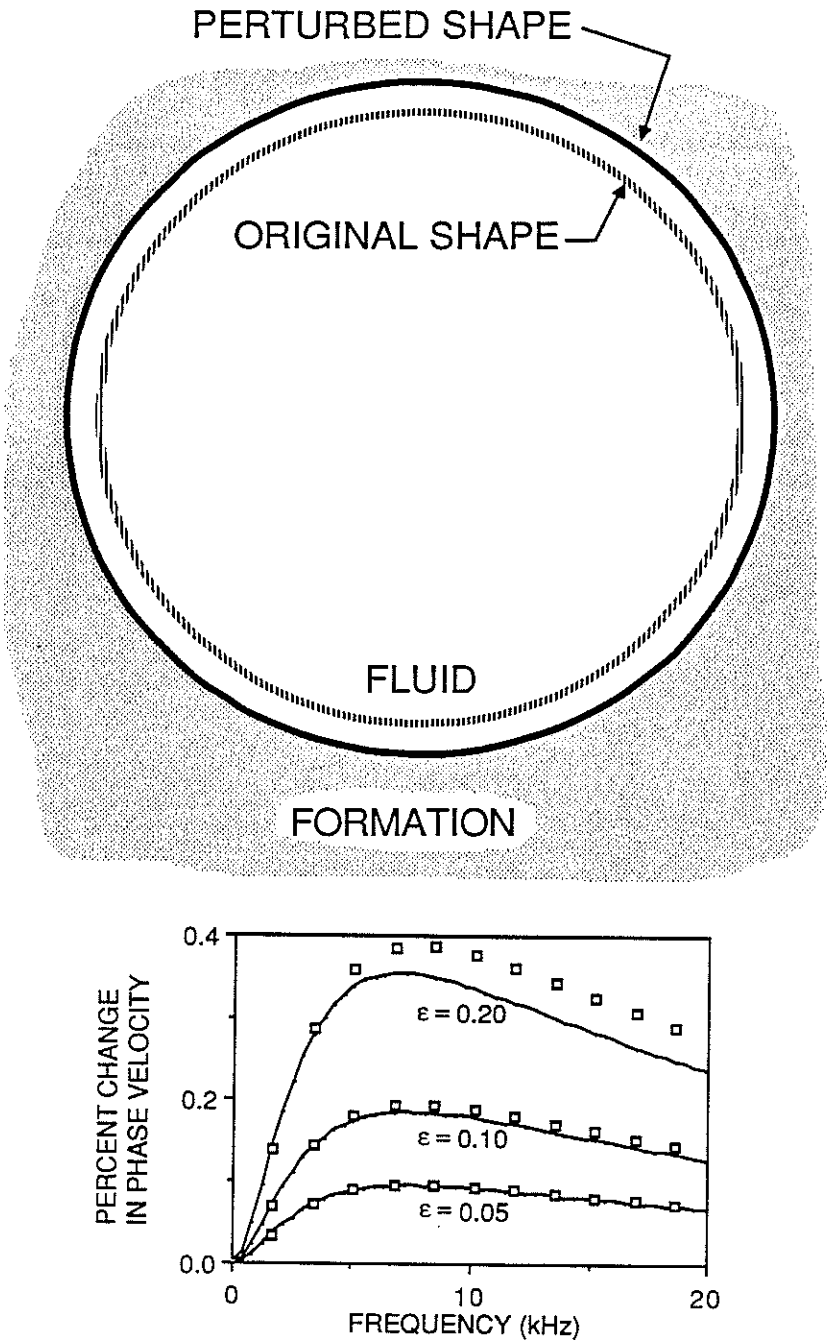

Figure 4: (a) Cross sections of two circular cylindrical boreholes with radii R and $R + \epsilon R$. These models were used to test the accuracy of the velocity corrections. (b) Percent change in the phase velocity of the tube wave for $\epsilon = 0.05$, 0.10, and 0.20. The solid line is the exact change, and the squares the change estimated with perturbation theory.

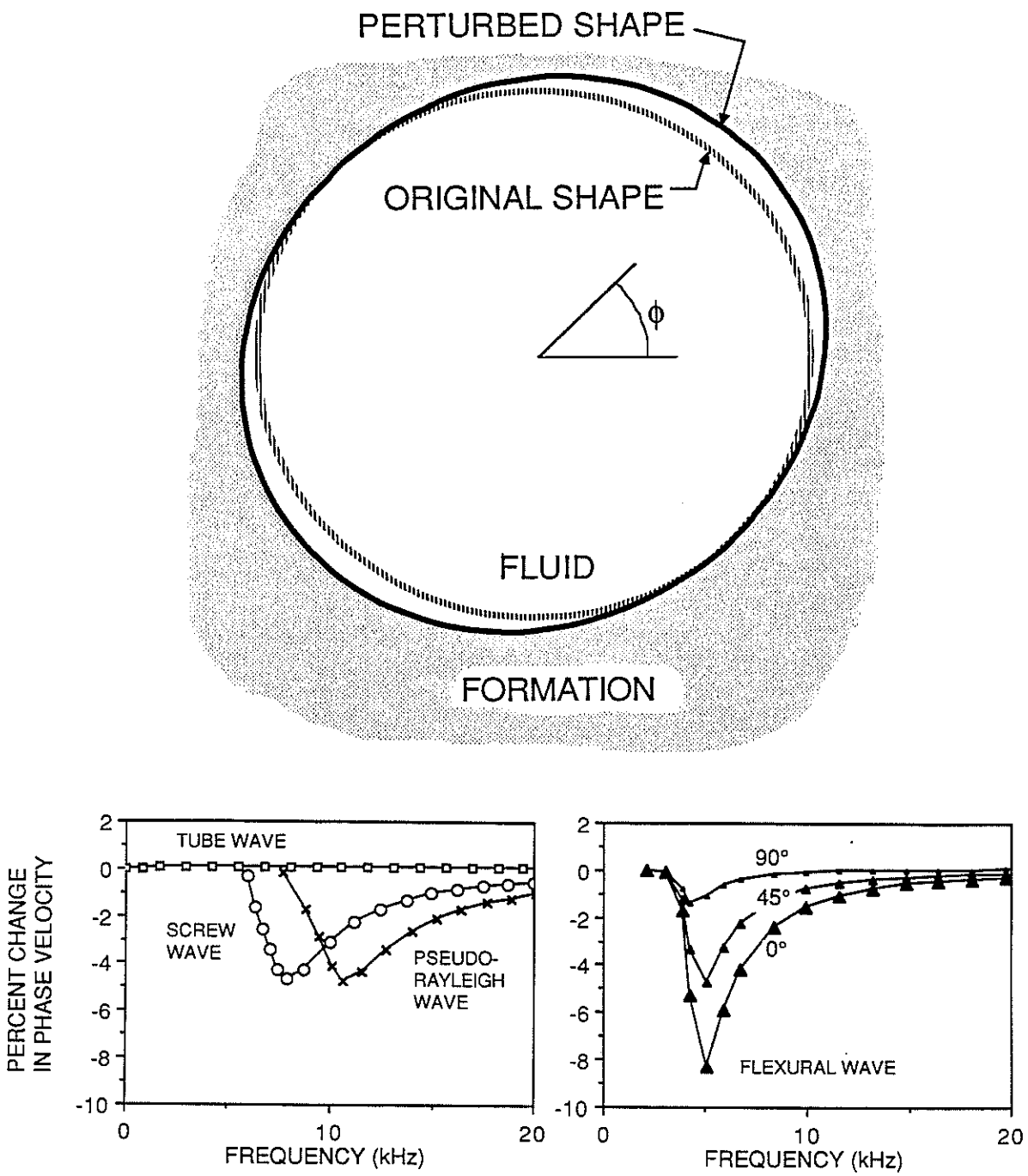

Figure 5: (a) Cross sections of the elliptical borehole and the original, circular borehole. (b) Percent change in the phase velocity of the tube, pseudo-Rayleigh, and screw waves due to the perturbation in the borehole wall. (c) Percent change in the phase velocity of the flexural wave for three orientations of the perturbation.

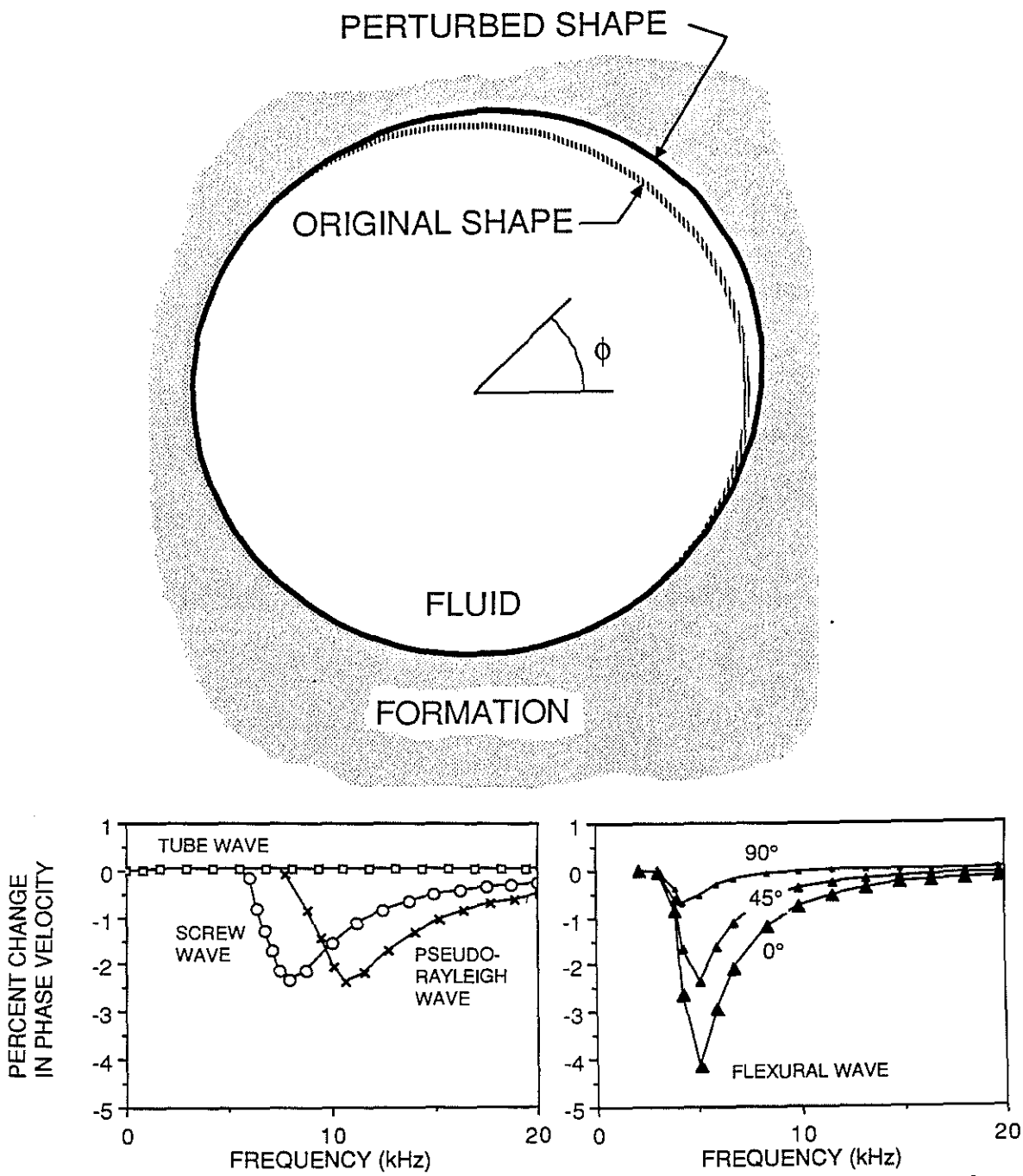

Figure 6: (a) Cross sections of the egg-shaped borehole and the original, circular borehole. (b) Percent change in the phase velocity of the tube, pseudo-Rayleigh, and screw waves due to the perturbation in the borehole wall. (c) Percent change in the phase velocity of the flexural wave for three orientations of the perturbation.

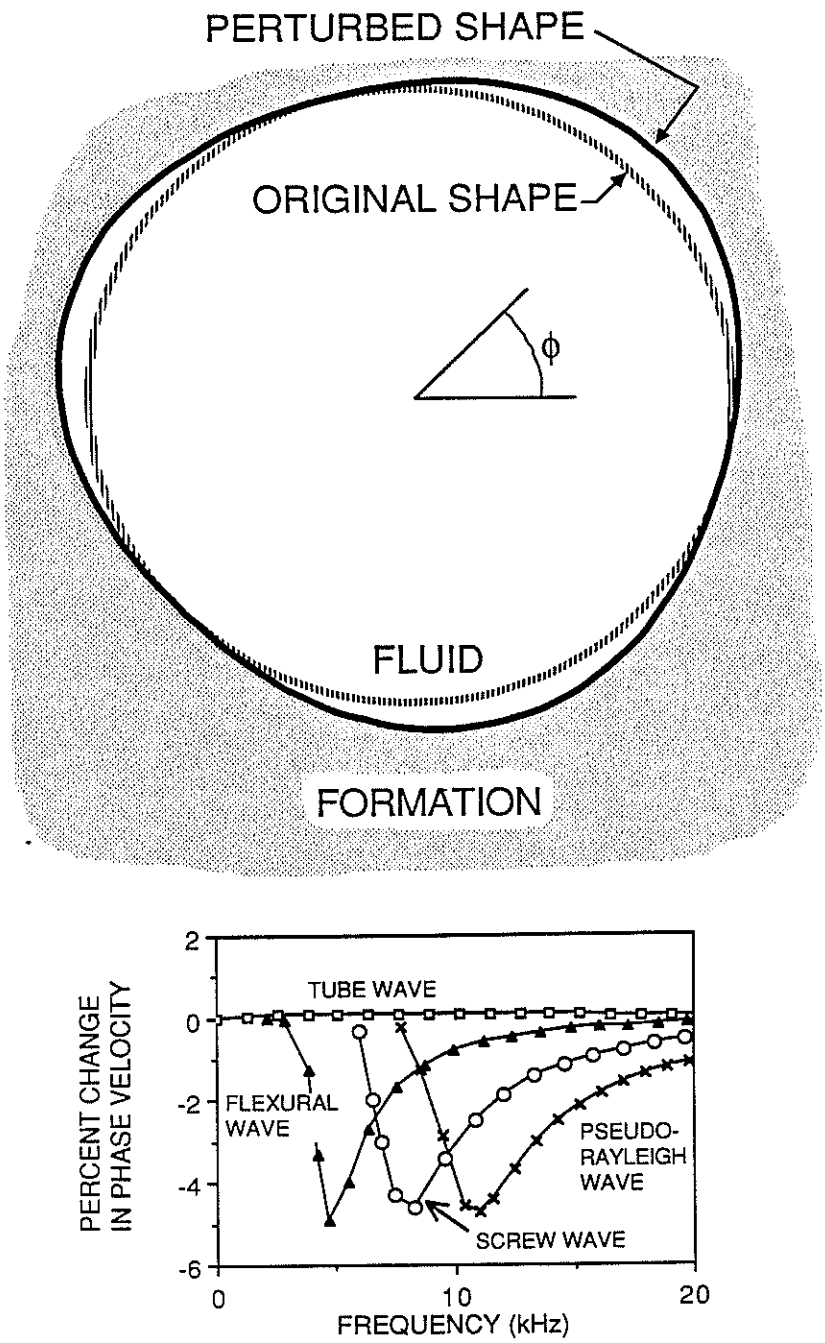

Figure 7: (a) Cross sections of the three-lobed borehole and the original, circular borehole. (b) Percent change in the phase velocity of the guided waves due to the perturbation in the borehole wall.